Effect of Water on Structure of Hydrophilic Imidazolium-Based Ionic Liquid

ARTICLE *in* THE JOURNAL OF PHYSICAL CHEMISTRY B · JULY 2009

Impact Factor: 3.3 · DOI: 10.1021/jp9042667 · Source: PubMed

Effect of Water on Structure of Hydrophilic Imidazolium-Based Ionic Liquid

Toshiyuki Takamuku,*,† Yasuhiro Kyoshoin,† Takuya Shimomura,† Shigeharu Kittaka,‡ and Toshio Yamaguchi§

Department of Chemistry and Applied Chemistry, Faculty of Science and Engineering, Saga University, Honjo-machi, Saga 840-8502, Japan; Department of Chemistry, Faculty of Science, Okayama University of Science, 1-1 Ridaicho, Okayama 700-0005, Japan; and Advanced Materials Institute and Department of Chemistry, Faculty of Science, Fukuoka University, Nanakuma, Jonan-ku, Fukuoka 814-0180, Japan

Received: May 7, 2009; Revised Manuscript Received: June 22, 2009

The state of water in room-temperature ionic liquid, 1-ethyl-3-methylimidazolium tetrafluoroborate ($EMI^+BF_4^-$), has been investigated by measurements of absorption and desorption isotherms, attenuated total reflectance infrared (ATR-IR) spectroscopy, and ^2H NMR relaxation method. The absorption enthalpies of water for the ionic liquid were estimated from the absorption isotherms. The enthalpies in the water mole fraction range of $x_w \leq \sim 0.5$ are lower than the enthalpy of vaporization for bulk water, but become larger than the value for bulk with increasing mole fraction of absorbed water. The ATR-IR spectra for $EMI^+BF_4^-$−water solutions in the range of $0.09 \leq x_w \leq 0.34$ have revealed that individual water molecules hydrogen-bonded to the anions predominate in the solutions at $x_w \leq \sim 0.2$, while ~30% of water molecules are hydrogen-bonded among them in the solutions at $x_w > \sim 0.3$. In addition, the activation energies for the rotational motion of a water molecule estimated from the ^2H NMR relaxation rates have indicated that the motion of water molecules in $EMI^+BF_4^-$−D_2O solutions gradually becomes freer with increasing water content from $x_w = 0.10$ to 0.30, but is retarded again at $x_w = 0.33$. Therefore, all the present findings have suggested that the state of water molecules in $EMI^+BF_4^-$ significantly changes at $x_w \approx 0.3$. On the other hand, to directly observe the effect of water on structure of $EMI^+BF_4^-$, LAXS experiments have been made on $EMI^+BF_4^-$−water solutions. It has been suggested that the interactions between the C_2 atom within the imidazolium ring of EMI^+ and BF_4^- are strengthened with increasing water content, while those at the C_4 and C_5 atoms weaken. Thus, the present LAXS experiments have clarified the beginning of formation of ion pair in $EMI^+BF_4^-$ by adding water at the molecular level.

Introduction

Room-temperature ionic liquids have been investigated as a novel solvent by many researchers in the fields of organic synthesis, extraction and separation, and electrochemistry because of their very low vapor pressure, nonflammability, high polarity, and electroconductivity. For the application of ionic liquids in such fields, they are frequently used with a cosolvent of conventional molecular liquid like water and acetonitrile. The physicochemical properties for mixtures of ionic liquid and molecular liquid, such as viscosity, conductivity, and polarity, depend on the mixing ratio of ionic liquid to molecular liquid.[1−7] However, the ratio is often determined by trial and error. On the other hand, trivial water absorbed into hydrophilic room-temperature ionic liquids from the atmosphere is a serious impurity. The impurity of water is difficult to remove from the hydrophilic ionic liquids because of the high hygroscopicity. Therefore, to progress the application for mixtures of ionic liquid and water as a novel solvent and to establish removal for trivial water as an impurity, state of water contained into ionic liquids at the molecular level is very important.

Many investigations on the state of water in room-temperature ionic liquids have been reported so far. Particularly, imidazolium-based ionic liquids have been a familiar subject for such studies. In the investigations, infrared (IR) spectroscopy is a powerful tool to directly observe the state of water in ionic liquids.[8−12] The interactions between 1-alkyl-3-methylimidazolium-based ionic liquids with various anions and water absorbed from the atmosphere were studied by using attenuated total reflectance infrared (ATR-IR) spectroscopy.[8] This showed that the interaction between anion and water molecules is a key of absorption of water for the ionic liquids. It was found that most of anions (X^-), such as tetrafluoroborate (BF_4^-) and hexafluorophosphate (PF_6^-), are bridged by one water molecule to form hydrogen-bonded species of $X^-\cdots HOH\cdots X^-$ in the ionic liquids. The energies of hydrogen bonds were estimated from spectral shift to be 8−13 kJ mol^{-1}. Recently, Zhang et al.[12] have made two-dimensional IR spectroscopic measurements on aqueous solutions of 1-ethyl-3-methylimidazolium (EMI^+) BF_4^- in the range of water mole fraction of $0.02 \leq x_w \leq 0.90$; the structure of EMI^+ is depicted in Figure 1 with the notation of atoms. They proposed a plausible dilution process of $EMI^+BF_4^-$ by water as follows. The inherent structure of $EMI^+BF_4^-$ is

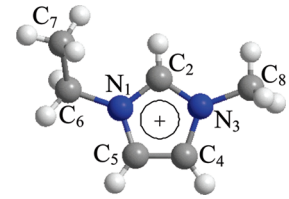

Figure 1. Structure of EMI^+ with notation of atoms.

* To whom correspondence should be addressed. E-mail: takamut@cc.saga-u.ac.jp.
† Saga University.
‡ Okayama University of Science.
§ Fukuoka University.

10.1021/jp9042667 CCC: $40.75
Published on Web 07/15/2009

gradually disturbed to ionic clusters when the amount of water is added, then the clusters further dissociate into ion pairs with increasing water content, and finally the ion pairs dominates in solutions. However, water molecules added do not completely separate $EMI^+BF_4^-$ to respective ions in the mole fraction range studied. It was also found that the stretching vibrations, C_2-H, C_4-H, C_5-H, $B-F$, appear to be constant at the lower water contents of $0.02 \leq x_w \leq 0.30$, while these remarkably change with increasing water content from $x_w = 0.30$ to 0.90. Thus, the structural change in $EMI^+BF_4^-$ may drastically take place at $x_w \approx 0.30$. NMR spectroscopy with nuclear Overhauser enhancement gave the evidence of interaction between 1-butyl-3-methylimidazolium (BMI^+) BF_4^- and water molecules.[13] Molecular dynamics (MD) simulations on aqueous solutions of 1,3-dimethylimidazolium chloride and PF_6^- showed that water monomers are formed in the solution at lower water contents than ionic liquid; on the contrary, water molecules are hydrogen-bonded with themselves in the solutions at higher water contents.[14]

As mentioned, many investigations have been done on the state of water in imidazolium-based ionic liquids. However, the thermodynamics for absorption of water molecules for ionic liquids has not yet been elucidated. In addition, structural change of the ionic liquid by addition of water has not been directly observed at the molecular level. We have studied the liquid structure of $EMI^+BF_4^-$ by using large-angle X-ray scattering (LAXS) technique with the help of MD simulations.[15] It has been revealed that liquid $EMI^+BF_4^-$ has a crystal-like structure; thus, anions of BF_4^- interact mainly with the imidazolium ring of EMI^+ at the C_2, C_4, and C_5 positions. The change in the inherent structure of $EMI^+BF_4^-$ by addition of water is of interest.

In the present study, we aimed at clarifying the structural change of $EMI^+BF_4^-$−water solutions at $x_w \approx 0.30$, which has been pointed out as a specific mole fraction by many researchers. First, absorption and desorption isotherms of water for dry $EMI^+BF_4^-$ were measured by weighing water absorbed as a function of vapor pressure of water up to the saturated pressure. In the measurements for weight of water absorbed, an electric balance connected to a vacuum line, which is generally used to investigate absorption and desorption of gas for porous materials, such as silica gel, could be applied because of the negligible vapor pressure of the ionic liquid. The absorption enthalpies of water for $EMI^+BF_4^-$ were estimated from the isotherms measured at various temperatures. ATR-IR spectroscopic measurements have been made on $EMI^+BF_4^-$−water solutions in the range of water mole fraction $0.09 \leq x_w \leq 0.34$, and the concentrations for both isolated water molecules interacting with the anions and hydrogen-bonded water aggregates in the solutions have been estimated from the ATR-IR spectra. Furthermore, ^2H NMR relaxation measurements have been performed on $EMI^+BF_4^-$−D_2O solutions in the same x_w range to elucidate the dynamics of water molecules in the ionic liquid. On the other hand, the change in the structure of $EMI^+BF_4^-$ by addition of water up to $x_w = 0.33$ has been observed by means of LAXS technique. Both state of water molecules in $EMI^+BF_4^-$ and structural change in the ionic liquid with increasing water content are discussed on the basis of all the present results.

Experimental Section

Sample Preparation. 1-Ethyl-3-methylimidazolium tetrafluoroborate ($EMI^+BF_4^-$, Nippon Synthetic Chemical Industry), whose melting point is 286 K,[16] was used after drying under vacuum at 313 K. The water content of $EMI^+BF_4^-$ was estimated to be less than 100 ppm by a Karl Fischer titration. Samples of $EMI^+BF_4^-$−water solutions for ATR-IR, ^2H NMR relaxation, and LAXS measurements were prepared by weighing dried ionic liquid and doubly distilled water or D_2O (Cambridge Isotope Laboratories, D content = 99.9%) to reach required mole fractions of water. In an aqueous solution, BF_4^- may slowly decompose by hydrolysis to give white turbidity. Thus, the $EMI^+BF_4^-$−water solutions prepared were used for all the experiments within 1 week. However, the turbidity was not observed in the present solutions for more than 1 month, and IR spectra for the solutions did not change.

Absorption and Desorption Isotherms. Absorption and desorption isotherms of water for $EMI^+BF_4^-$ at 283, 291, 298, and 303 K were measured by using an electronic balance (BEL, Rubotherm) connected to a vacuum line. The vapor pressure of water in the vacuum line was measured by a capacitance manometer (MKS Baratron, type 390H) linked to a personal computer. The weight of the sample solution at each vapor pressure of water was measured at long intervals (3−4 h) to reach equilibrium.

ATR-IR Spectroscopy. ATR-IR measurements with a single reflectance on $EMI^+BF_4^-$−H_2O solutions at $x_w = 0.09$, 0.17, 0.23, 0.26, 0.29, and 0.34 were made at a room temperature by using an FT-IR spectrometer (JASCO, FT/IR-6100) with ATR diamond prism (JASCO, PKS-D 470 with ATR PRO450-S). During the measurements, the light path in the spectrometer was purged with dry N_2 gas at flow rate of 5 $dm^3\ min^{-1}$ to eliminate moisture and carbon dioxide. The absorption spectra were accumulated for 128 times per sample with a resolution of 4.0 cm^{-1}. In the ATR-IR spectroscopy, the absorption occurs in the evanescent wave penetrating into the sample, resulting in a decrease in the amplitude of irradiated light. The penetration depth d_p of the evanescent wave per reflection by a prism can be estimated through[17]

$$d_p = \frac{\lambda}{2\pi}(n_1\sqrt{\sin^2\theta - n_2^2/n_1^2})^{-1} \quad (1)$$

Here, λ represents the wavelength of the light, θ is the incident angle (45°) and n_1 and n_2 give the refractive indexes of diamond prism (2.42) and sample solution, respectively. Thus, the wavelength dependence of the penetration depth must be corrected to exactly determine a peak area for each absorption band. In the present experiments, the reflective indexes for the samples at 298 K were determined by using a digital Abbe refractometer (ATAGO, DR-A1) to correct the path length of the light for the spectra.

^2H NMR Relaxation. ^2H spin−lattice times T_1 of $EMI^+BF_4^-$−D_2O solutions at $x_{D_2O} = 0.10$, 0.17, 0.23, 0.29, and 0.33 were measured in the temperature range from 253 to 313 K with an FT-NMR spectrometer (JEOL, JNM-AL300). For comparison, T_1 for pure D_2O was also measured in the range from 278 to 308 K. The resonance frequency of ^2H atom was 42.11 MHz. The sample solution was kept into a 5 mm sample tube (Shigemi, PS-001), and its temperature required was kept constant within ±0.1 K by mixtures of hot air and a cold nitrogen stream generated from liquid nitrogen. T_1 was measured by the inversion-recovery method with a pulse sequence $(\pi-\tau-\pi/2)^n$, where the number n of the delay times τ in the series of the sequence was 13. The longest delay time exceeded $5T_1$. The T_1 values for each sample solution were measured three times at least and averaged to give a final value.

LAXS Experiments. LAXS measurements at 298 K were performed on pure $EMI^+BF_4^-$ and its H_2O solutions at $x_w =$

0.10 and 0.33. A rapid liquid X-ray diffractometer (Bruker AXS, DIP 301) with an imaging plate (IP) (Fuji Film Co.) as a two-dimensional detector was used in the present LAXS experiments. Details of the diffractometer have been described in the literature.[18,19] X-rays were generated at a rotary Mo anode (Rigaku, RU-300) operated at 50 kV and 200 mA and monochromatized by a flat graphite crystal to obtain Mo Kα radiation (wavelength $\lambda = 0.7107$ Å). The sample solution was sealed into a glass capillary (W. Müller Co.) of 2 mm inner diameter with wall thickness of 0.01 mm during measurements. The scattering intensities for the sample solution were accumulated on the IP for 1 h, and those for an empty capillary were also measured as background. The observed range of the scattering angle (2θ) was 0.2°−109°, corresponding to the scattering vector s ($= 4\pi\lambda^{-1} \sin\theta$) of 0.03−14.4 Å^{-1}. Densities of the sample solutions were measured at 298 K by using densimeter (Anton Paar K.G., DMA60 and DMA602) for analysis of LAXS data.

First, two-dimensional X-ray data measured on the IP were corrected for polarization and then integrated to obtain one-dimensional data.[18] Then, the intensities for the samples and empty capillary were corrected for absorption.[19] The contribution of the sample solution alone was obtained by subtracting the intensities for empty capillary from those for the sample. Finally, the corrected intensities were normalized to absolute units by conventional methods.[20−22] The structure function, $i(s)$, for the sample solution was obtained as previously reported[23] and then Fourier transformed into the radial distribution function, $D(r)$, in a usual manner.[23]

To make a quantitative analysis on the X-ray data, a comparison between experimental structure function and theoretical one calculated on a structure model was made by a least-squares refinement procedure through eq 5 in ref 23. In the data treatment, the stoichiometric volume V was chosen to contain one EMI^+ in the solutions. These data treatments were made by using programs KURVLR[24] and NLPLSQ.[25]

Results and Discussion

Absorption and Desorption Isotherms. Since the vapor pressure of $EMI^+BF_4^-$ is negligible, the ionic liquid is permitted to stand under a vacuum. Thus, we tried to measure absorption and desorption isotherms of water for the ionic liquid as a function of water vapor pressure by using an electric balance connected to a vacuum line. Figure 2a shows the absorption isotherms of water for $EMI^+BF_4^-$ at 283, 291, 298, and 303 K and the desorption one at 298 K. The sample of $EMI^+BF_4^-$ at 283 K is in a supercooled state due to the melting point of 286 K.[16] At each temperature the mole fraction of water absorbed gradually increases when the vapor pressure of water increases, indicating that water is monotonously absorbed to $EMI^+BF_4^-$ with increasing vapor pressure of water. At 298 K the desorption isotherm almost overlaps with the absorption one, although the former at lower pressures slightly deviates from the latter due probably to the uncertainties for the low pressure measurements. This result shows that absorption and desorption of water for $EMI^+BF_4^-$ reversibly take place as a function of water vapor pressure. In Figure 2b, the absorption and desorption isotherms are replotted against the relative vapor pressure of water to the saturated one at each temperature. The changes in the isotherms at all the temperatures studied overlap among them. Thus, the absorption of water for $EMI^+BF_4^-$ depends only on the vapor pressure of water in the present temperature range, which includes the melting point of 286 K.

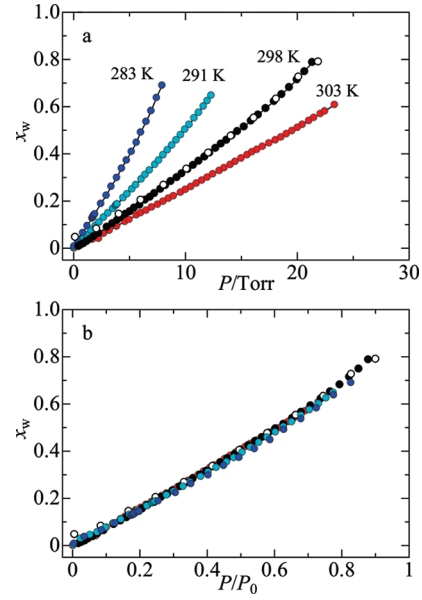

Figure 2. Absorption and desorption isotherms of water for $EMI^+BF_4^-$ at various temperatures as a function of (a) water vapor pressure and (b) relative water pressure to the saturated one. Filled and open circles represent absorption and desorption, respectively.

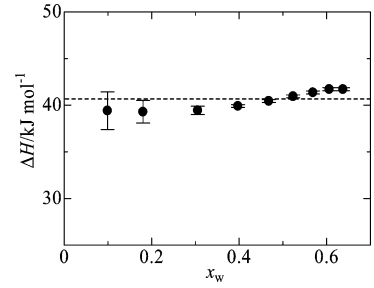

Figure 3. Absorption enthalpies of water for $EMI^+BF_4^-$ as a function of mole fraction of water absorbed. Dashed line gives the enthalpy of vaporization for bulk water at 298 K. The standard deviations σ are indicated as error bars.

To estimate the absorption enthalpies of water for $EMI^+BF_4^-$, the Clausius−Clapeyron equation was applied to the relation between the temperatures and the vapor pressures at equimolar water contents, which were determined from the absorption isotherms. In Figure 3, the absorption enthalpies of water estimated are depicted as a function of mole fraction of water absorbed, together with the enthalpy of vaporization for bulk water at 298 K as the dashed line. As seen in the figure, the absorption enthalpies in the low mole fraction range of $x_w \leq \sim 0.3$ are lower than that of vaporization for bulk water. However, they are gradually close to the value for bulk water with increasing water mole fraction and become larger beyond that for bulk in the range of $x_w > \sim 0.5$. It thus results in an inflection point at $x_w \approx 0.5$. This finding suggests that the state of water absorbed for $EMI^+BF_4^-$ changes at $x_w \approx 0.5$; i.e., water molecules in the range of $x_w < \sim 0.5$ are weakly absorbed into the ionic liquid, while they are tightly absorbed at $x_w > \sim 0.5$.

ATR-IR Spectroscopy. Figure 4 shows IR spectra for the $EMI^+BF_4^-$−H_2O solutions in the wavenumber range from 2700 to 3800 cm^{-1}, which were corrected for the wavelength dependence of the path length using eq 1. Several bands assigned to the C−H vibrations within EMI^+ are observed in the range of 2800−3300 cm^{-1}; sharp and large peaks at 3124 and 3165 cm^{-1} are attributed to the C_2−H and $C_{4,5}$−H vibrations within the imidazolium ring, respectively, and smaller peaks in the

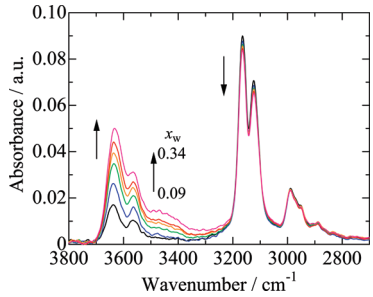

Figure 4. ATR-IR spectra of $EMI^+BF_4^-$−H_2O solutions as a function of water mole fraction. The arrows indicate the change in the mole fraction from $x_w = 0.09$ to 0.34.

range from 2800 to 3020 cm^{-1} arise from various C−H vibrations within both methyl and ethyl groups.[26] These are in disagreement with the previous ATR-IR study on $EMI^+BF_4^-$−D_2O solutions; the C_2−H and $C_{4,5}$−H vibrations of the imidazolium ring appear at 3074 and 3152 cm^{-1} in the previous spectrum.[12] In particular, no peak appears at 3074 cm^{-1} in the present spectra. However, the peak positions for both vibrations observed in the present spectra agree well with those for pure $EMI^+BF_4^-$ and $BMI^+BF_4^-$ reported by Katsyuba et al.[26] and Jeon et al.,[11] respectively. In the whole x_w range studied, the peak positions of both C_2−H and $C_{4,5}$−H vibrations scarcely change. Although the positions for both vibrations observed in the present study differ from those in the previous one on $EMI^+BF_4^-$−D_2O solutions,[12] this tendency agrees with each other. It is thus suggested that the interactions of the imidazolium ring with BF_4^- do not drastically change from the inherent ones in pure liquid by addition of water in this x_w range.

On the other hand, two peaks at 3565 and 3638 cm^{-1} observed for the $EMI^+BF_4^-$−H_2O solutions are assigned to the symmetric and antisymmetric O−H stretching vibrations, ν_s and ν_{as}, within an isolated water molecule interacting with the anions, respectively.[9,10,12] When the water content increases, a broad peak at 3450 cm^{-1} arising from the O−H vibration of hydrogen-bonded water molecules, ν_{HB}, appears.[9] The three peaks assigned to the O−H vibrations of water molecules were fitted by using a pseudo-Voigt function consisting of Lorentzian and Gaussian to deconvolute them into each component. The results of fits showed no significant shift of each peak with increasing water content. The amounts of the isolated water molecules interacting with the anions and the hydrogen-bonded water aggregates in the $EMI^+BF_4^-$−H_2O solutions were estimated from the areas for ν_{as} and ν_{HB} bands, respectively. First, the molar absorption coefficient for the ν_{as} band was determined from the spectrum for the solution at $x_w = 0.09$ on the first approximation that no water molecules form hydrogen bonds with themselves. Actually, the area for ν_{HB} band in the spectrum at the mole fraction is negligible. Then, the molarities for the isolated water molecules were estimated from the area for the ν_{as} band of the solutions at the other mole fractions by using the molar absorption coefficient determined. On the other hand, the tentative values for the hydrogen-bonded water aggregates could be obtained by subtracting the molarity for the isolated water molecules from that for the total water. Then, the final values were estimated from the area for the ν_{HB} band and its molar absorption coefficient determined by averaging the respective coefficients for the solutions obtained from the tentative molarity for the hydrogen-bonded water aggregates so that the final and tentative molarities agreed with each other within the uncertainty of ~10%.

Figure 5 shows the concentrations for the isolated water molecules interacting with the anions and the hydrogen-bonded water aggregates estimated for the $EMI^+BF_4^-$−H_2O solutions as a function of water mole fraction. The concentration for the isolated water molecules monotonously increases with increasing x_w. On the other hand, the concentration for the hydrogen-bonded water molecules rises above $x_w = 0.23$, although very small in the range of $x_w \leq 0.2$. Thus, water molecules tend to aggregate significantly in the $EMI^+BF_4^-$−H_2O solutions when the mole fraction reaches $x_w \approx 0.23$. The figure shows that ~0.9 mol dm^{-3} of water molecules in the total water concentration of 3.2 mol dm^{-3} form hydrogen bonds among them in the solution at $x_w = 0.34$; i.e., ~30% of water molecules aggregate through hydrogen bonds in $EMI^+BF_4^-$. The present results from the IR spectra, together with the inflection point at $x_w \approx 0.5$ observed in the absorption enthalpies of water, suggest that the change in the state of water undergoes in the ionic liquid above $x_w \approx 0.3$.

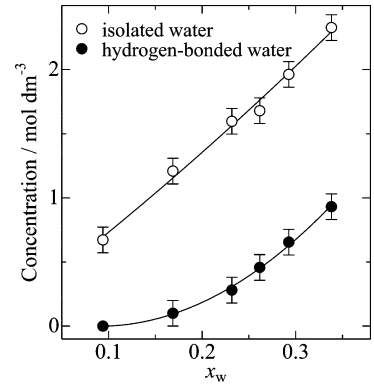

Figure 5. Molarities of isolated water molecules interacting with BF_4^- (open circles) and hydrogen-bonded water aggregates (closed ones) for $EMI^+BF_4^-$−H_2O solutions as a function of water mole fraction. Solid lines are depicted for clarification of the change in the molarities with mole fraction. The standard deviations σ are indicated as error bars.

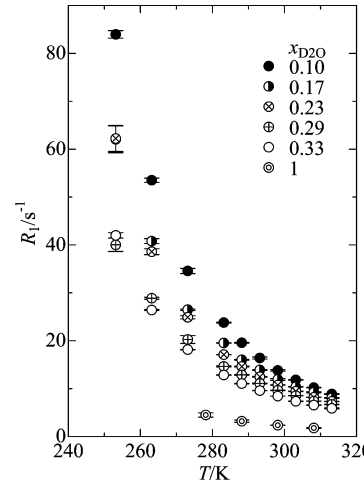

Figure 6. ^2H NMR relaxation rates R_1 for D_2O ($x_w = 1$) and $EMI^+BF_4^-$−D_2O solutions at various water mole fractions in the temperature range from 253 to 313 K. The standard deviations σ are indicated as error bars.

^2H NMR Relaxation. Figure 6 reveals the ^2H NMR relaxation rates ($R_1 = T_1^{-1}$) for the $EMI^+BF_4^-$−D_2O solutions at various D_2O mole fractions as a function of temperature in the range from 253 to 313 K, where the melting point 286 K of $EMI^+BF_4^-$ is included.[16] Those for pure D_2O ($x_{D_2O} = 1$) in the range from 278 to 308 K are also depicted in the figure for comparison. The ^2H relaxation rate is related to the rotational correlation time of D_2O molecules as described in the literature; the relaxation rate increases if the rotational motion of D_2O

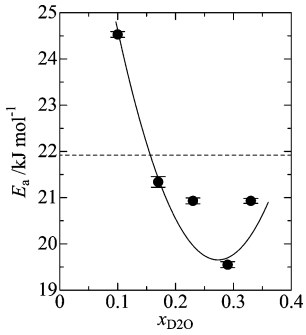

Figure 7. Activation energies E_a of the rotational motion for water molecules as a function of water mole fraction. Dashed line represents the E_a for pure D_2O, and the solid line is depicted for clarification of the change in the energies with mole fraction. The standard deviations σ are indicated as error bars.

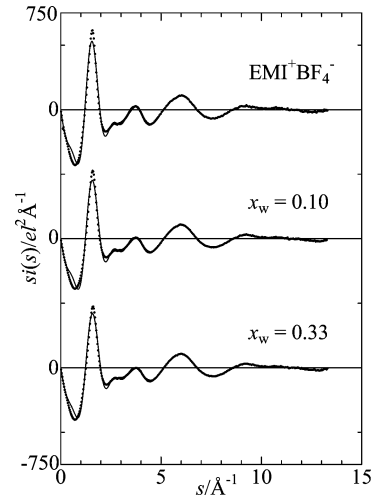

Figure 8. Structure function $i(s)$ weighted by s for $EMI^+BF_4^-$ and $EMI^+BF_4^-$−H_2O solutions at $x_w = 0.10$ and 0.33. Dotted lines represent experimental values, and solid lines are theoretical ones.

molecules is restricted by perturbation, such as temperature and pressure.[27] As seen in Figure 6, the R_1 values for the $EMI^+BF_4^-$−D_2O solutions are much larger than that for pure D_2O over the present temperature range, showing that the rotational motion of water molecules is retarded in $EMI^+BF_4^-$. Moreover, the mole fraction dependence of the restriction for the rotational motion at each temperature is more significant at the lower temperatures, particularly below the melting point. It is shown that the rotational motion of isolated water molecules is easily restricted in $EMI^+BF_4^-$ by cooling because the structure of $EMI^+BF_4^-$ becomes gradually rigid with lowering temperature.

The activation energies for the rotational motion of water molecules in pure D_2O and the $EMI^+BF_4^-$−D_2O solutions were estimated by Arrhenius plots for the rotational correlation times τ_{2R} determined from the R_1 values in the high-temperature range from 283 to 313 K in accordance with the extreme narrowing condition ($\omega_0\tau_{2R} \ll 1$, where ω_0 is the resonance frequency of ^{2}H atom).[28] In the estimation, the quadrupole coupling constant QCC (254 kHz) and the asymmetry parameter η (0.135) for liquid D_2O were adopted.[29] Although the QCC should depend on the composition of solution and temperature, the QCC value for each solution and temperature is not available in the literature. Struis et al. investigated a dependence of QCC value of D_2O on the intramolecular O−D distance.[29] They reached the conclusion that the value hardly changes in the wide temperature range of 278−326 K. The recent ^{2}H NMR relaxation investigation on D_2O in BMI^+Cl^- and $BMI^+PF_6^-$ using two spectrometers with different resonance frequencies gave smaller QCCs (142 and 89 kHz, respectively) by a factor of 2−3 than that for liquid D_2O.[30] It was also reported that the QCCs do not remarkably depend on the water content and temperature though the values vary by anions. Despite the variation of QCCs, the slope in the Arrhenius plots is independent of the QCCs, when the constant value is used for all the solutions. Thus, the constant QCC for liquid D_2O was utilized in the present estimation. In the temperature range of 283−313 K examined, the τ_{2R} values for the $EMI^+BF_4^-$−D_2O solutions below $x_{D_2O} = 0.33$ were estimated to be 6.5−25 ps. Thus, the $\omega_0\tau_{2R}$ values for the solutions at $\omega_0 = 42.11$ MHz $= 2.646 \times 10^8$ rad s^{-1} in the present experiments are adequately smaller than unity. The τ_{2R} values fall into the range of 53−206 ps even if the smallest QCC (89 kHz)[30] for D_2O in $BMI^+PF_6^-$ among the known is applied; thus, the $\omega_0\tau_{2R}$ value is still satisfactorily smaller than unity. Hence, the extreme narrowing condition is applicable for the present solutions.

In Figure 7, the activation energies for the rotational motion of water molecules are plotted as a function of D_2O mole fraction. The E_a value for pure D_2O was estimated to be 21.92 ± 0.04 kJ mol^{-1} as depicted by the dashed line. The value for pure D_2O is comparable with that (22.5 kJ mol^{-1}) previously reported.[31] Figure 7 indicates that the E_a value for the $EMI^+BF_4^-$−D_2O solution at $x_{D_2O} = 0.10$ is much larger than that for bulk, suggesting that the rotational motion of water molecules is strongly restricted in the inherent structure of $EMI^+BF_4^-$ due to the bridged-structure of $BF_4^-\cdots DOD\cdots BF_4^-$ by hydrogen bonding.[8] When the x_{D_2O} increases to 0.29, the E_a value gradually decreases below that for bulk. The addition of water molecules may cause the loosening of the structure of $EMI^+BF_4^-$. Hence, the rotational motion of isolated water molecules accommodated in the structure of the ionic liquid becomes freer than that of water molecules in the bulk. However, the E_a value for the solution at $x_{D_2O} = 0.33$ increases again toward that for bulk. This is ascribed to the formation of water aggregates by hydrogen bonds, resulting in the remarkable restriction of the rotational motion of water molecules. The ^{2}H NMR relaxation results are in agreement with those from the absorption isotherm and ATR-IR spectroscopic measurements; i.e., the state of water molecules in the $EMI^+BF_4^-$−D_2O solutions changes at $x_{D_2O} \approx 0.3$. Thus, the isolated water molecules, which weakly interact with BF_4^-, are dominant in inherent structure of $EMI^+BF_4^-$ below $x_{D_2O} \approx 0.3$, but hydrogen bonds among water molecules significantly form in the solutions above $x_{D_2O} \approx 0.3$.

LAXS Experiments. The s-weighted structure function $i(s)$ for pure $EMI^+BF_4^-$ is depicted in Figure 8, and the corresponding radial distribution function (RDF) in the form of $D(r) - 4\pi r^2\rho_0$ obtained by Fourier transformation for the structure function is displayed in Figure 9. As reported in the previous study,[15] prominent peaks at 1.4 and 2.3 Å in the RDF for $EMI^+BF_4^-$ are attributed to the intramolecular interactions within EMI^+ and BF_4^-; the first peak is assigned to the C−C, C−N, and B−F bonds, while the second one arises from nonbonding interactions of C···C, C···N, and F···F. The broad and large band in the r-range from 3 to 6 Å is mainly ascribed to intermolecular interactions between EMI^+ and BF_4^-, and intramolecular interactions of EMI^+ in the longer range also contribute to the band.[15] To determine structure parameters of $EMI^+BF_4^-$, such as atomic distances r and coordination numbers n, a model fit was made on the RDF for $EMI^+BF_4^-$ on the basis of the previous results from the MD simulations.[15] The structure parameters of the intramolecular interactions of EMI^+ and BF_4^-

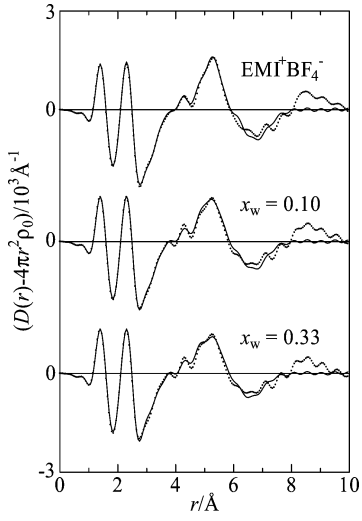

Figure 9. RDFs in the form of $D(r) - 4\pi r^2\rho_0$ for $EMI^+BF_4^-$ and $EMI^+BF_4^-$−H_2O solutions at $x_w = 0.10$ and 0.33. Dotted lines represent experimental values, and solid lines are theoretical ones.

are set in accordance with the crystal structure of $EMI^+BF_4^-$[32,33] and summarized in Table S1 in the Supporting Information. As previously reported,[34] EMI^+ exist in an equilibrium between planar and nonplanar conformers, where the ethyl group is at the same plane of the imidazolium ring and stands up from the plane with the dihedral angle $C_2N_1-C_6C_7$ of 110°, respectively. In the present analysis, thus, the planar and nonplanar conformers at the concentration ratio of 6:4 were assumed for the intramolecular interactions within EMI^+; however, only nonplanar conformer was considered to fit the intermolecular interactions between EMI^+ and BF_4^- for simplification. In fact, the RDFs obtained from the previous MD simulations with the respective models for planar and nonplanar EMI^+ were not remarkably different from each other.[15] A plausible structure model for interactions between EMI^+ and BF_4^- was built up to explain the RDF for $EMI^+BF_4^-$ in the range of $r \leq \sim 6$ Å. Instead of the longer-range interaction beyond ~6 Å, continuum electron distribution for each atom was assumed. To optimize the structure parameters, the structure function calculated by using the parameter values modeled was compared with the observed one in the s-range from 0.1 to 13.3 $Å^{-1}$ by using a least-squares refinement procedure. All the values determined are summarized in Table S2 in the Supporting Information, and the important parameter values optimized are extracted in Table 1. As seen in Figures 8 and 9, the theoretical $si(s)$ and RDF calculated by using the structure parameter values in Tables S1 and S2 well reproduce the observed ones in the ranges of $s \geq \sim 2$ $Å^{-1}$ and $r \leq \sim 6$ Å, respectively, where the model fitting was made in the present analysis.

The structure model obtained is illustrated in Figure 10 with important atomic distances. In the model, two BF_4^- interact with the C_2 atom from both upper and lower sides of the imidazolium ring, and two other BF_4^- are close to the C_4 and C_5 atoms, respectively. This geometry of BF_4^- around EMI^+ is compared to the crystal structure of $EMI^+BF_4^-$ determined by X-ray diffraction experiments,[32,33] suggesting that the crystal-like structure is kept even in the liquid state. As seen in Figure 10, linear hydrogen bonds of C−H···F between the imidazolium hydrogen atoms and F atoms of BF_4^- do not form. Thus, the C−H vibrations in the imidazolium ring are not sensitive to the change in the structure of the ionic liquid by addition of water, as described above. The closest F atom of BF_4^- interacts with the C_2 atom of the imidazolium ring with the distance of

TABLE 1: Important Optimized Parameter Values of the Interactions in $EMI^+BF_4^-$ and $EMI^+BF_4^-$−H_2O Solutions by Least-Squares Fits[a]

			$EMI^+BF_4^-$−H_2O	
interaction	parameter	$EMI^+BF_4^-$	$x_w = 0.10$	$x_w = 0.33$
	Interactions between EMI^+ and BF_4^-			
$C_2\cdots B_{1,2}$	r	3.63	3.62	3.59
	10^3b	20	15	15
	n	2.0	2.0	2.0
$C_2\cdots F_{14,21}$	r	2.90(1)	2.85(1)	2.84(1)
	10^3b	10	10	10
	n	2.0(2)	2.0(1)	1.9(1)
$C_2\cdots F_{12,22}$	r	3.19	3.19	3.19
	10^3b	20	10	10
	n	2.0	2.0	2.0
$C_2\cdots F_{11,24}$	r	4.57	4.58	4.56
	10^3b	25	25	25
	n	2.0	2.0	2.0
$C_2\cdots F_{13,23}$	r	4.60	4.56	4.54
	10^3b	25	25	25
	n	2.0	2.0	2.0
$C_{5,4}\cdots B_{3,4}$	r	3.87	3.87	3.87
	10^3b	20	20	25
	n	2.0	2.0	2.0
$C_{5,4}\cdots F_{32,34,41,43}$	r	3.44(1)	3.42(1)	3.42(1)
	10^3b	20	20	25
	n	3.9(2)	4.1(2)	3.9(2)

[a] The interatomic distance r (Å), the temperature factor b ($Å^2$), and the number of interaction n. The values in parentheses are standard deviations of the last figure. The parameters without standard deviations were not allowed to vary in the calculations.

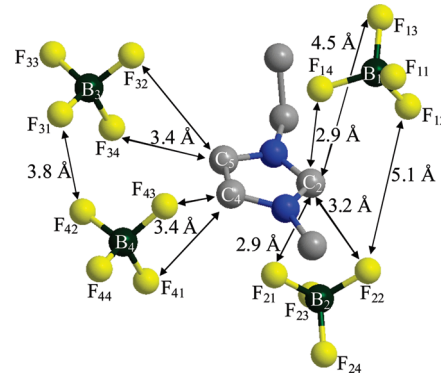

Figure 10. Structure model of interactions between EMI^+ and BF_4^-. Hydrogen atoms of EMI^+ are omitted for clarity.

~2.9 Å, and the distance between the other F atom of the same BF_4^- and the C_2 atom is estimated to be ~3.2 Å. Two other F atoms far from the imidazolium ring are apart from the C_2 atom with the distance of ~4.6 Å. On the other hand, two F atoms of BF_4^- equally interact with the C_4 and C_5 atoms in the imidazolium ring with the distance of ~3.4 Å. The distances between two other F atoms and the C_4 or C_5 atoms are ~4.1 and ~5.2 Å, respectively. The present LAXS results show that the C···F interactions mainly exist at the three distances of ~3.1, ~4.6, and ~5.2 Å. This is consistent with the previous results;[15] i.e., the C···F interactions were significantly observed at 3.4, 4.4, and 5.5 Å in the atom−atom pair correlation functions obtained by the MD simulations.

Figures 8 and 9 also show the structure functions and RDFs, respectively, for the $EMI^+BF_4^-$−H_2O solutions at $x_w = 0.10$ and 0.33. The RDFs for the solutions at the mole fractions mainly give information on interactions among EMI^+ and BF_4^- because the molarities of water are low due to the much larger molecular volume of $EMI^+BF_4^-$; in particular, information on

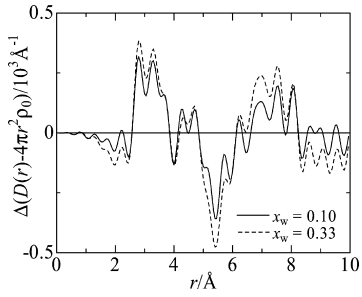

Figure 11. Differential RDFs for $EMI^+BF_4^-$−H_2O solutions at x_w = 0.10 (solid line) and 0.33 (dashed line) obtained by subtracting the RDF for $EMI^+BF_4^-$ from the original RDFs for $EMI^+BF_4^-$−H_2O solutions.

water molecules is scarce in the RDF at x_w = 0.10. A comparison between the RDFs for the solutions and pure ionic liquid reveals that the inherent structure of $EMI^+BF_4^-$ does not drastically change by adding water at the mole fractions. However, the large peak centered at 5.2 Å slightly weakens with increasing water content. To clarify the change in the RDF with increasing water content, the differential RDFs (DRDFs) were calculated by subtracting the RDF for pure $EMI^+BF_4^-$ from those for the $EMI^+BF_4^-$−H_2O solutions with taking into account the difference between both concentrations. Figure 11 indicates the DRDFs for the $EMI^+BF_4^-$−H_2O solutions at x_w = 0.10 and 0.33. The peaks centered at 3 and 4.5 Å increase with increasing water content, while the valley at 5.2 Å becomes deeper. According to the structure of pure $EMI^+BF_4^-$ as discussed above, the increase in the broad peaks at 3 and 4.5 Å suggests that the interactions between the C_2 atom and the closest F atom of BF_4^- are strengthened by addition of water. This leads to the strengthening of the interactions between the C_2 atom and the other F atom of the same BF_4^-. The interactions between the C_4 and C_5 atoms and the F atom of BF_4^- might contribute to the strengthened peak at 3 Å in the DRDFs. In practice, however, the interactions weaken by addition of water, because the deepening of the valley at 5.2 Å suggests that the interactions between the C_4 and C_5 atoms and the other F atoms far from the ring become weaker. These findings in the DRDFs reveal that the interaction between the C_2 atom and BF_4^- strengthens by addition of water, whereas interactions at the C_4 and C_5 atoms weaken. As shown in the crystal structure of $EMI^+BF_4^-$,[32,33] two BF_4^- around the C_4 and C_5 atoms also interact with the C_2 atom of the neighbor imidazolium ring. This may be the same in the liquid state. Thus, the present LAXS results suggest the decrease in the number of BF_4^- around EMI^+ by addition of water; i.e., the beginning of formation of ion pair EMI^+ and BF_4^- is observed in $EMI^+BF_4^-$ at the low water contents. The results from the ATR-IR measurements in Figure 5 demonstrated that about one-third of water molecules form aggregates by hydrogen bonding in the $EMI^+BF_4^-$−H_2O solutions above $x_w \approx 0.3$. Probably, the aggregates of water molecules would play a role as a wedge to break the inherent structure of $EMI^+BF_4^-$ because of weak interactions between water molecules and both cation and anion. Thus, it is expected that the DRDF at x_w = 0.33 includes the information of water aggregates by hydrogen bonds; however, since the first- and second-neighbor interactions at 2.8 and 4.5 Å in the tetrahedral-like structure of water are superimposed in the large broad peaks at 3 and 4.5 Å due mainly to the interactions between the C_2 atom in the imidazolium ring and the F atoms of BF_4^-, it was not possible to make a quantitative analysis of the water aggregates in the DRDF. The peak at 7 Å assigned to the third-neighbor O···O interactions in the tetrahedral-like water structure significantly strengthens at x_w = 0.33.

To make a quantitative analysis on the change in the structure of $EMI^+BF_4^-$−H_2O solutions by addition of water, model fits were performed on the RDFs for the solutions by modifying the parameters determined for pure $EMI^+BF_4^-$, together with continuum electron distribution for each atom included in the solutions. The intramolecular interactions for $EMI^+BF_4^-$ and water[35] utilized for the fits are listed in Table S1 in the Supporting Information. To refine the parameter values modeled, a least-squares procedure was applied to compare the theoretical structure function calculated by using the parameter values modeled with the observed one. In Table 1, the important parameter values optimized are shown, and all the optimized values are listed in Table S2 in the Supporting Information. Figures 8 and 9 reveal that the theoretical values in both *s*- and *r*-spaces calculated by using the optimized parameter values in Tables S1 and S2 well reproduce the observed ones, respectively. As seen in Table 1, the distance between the C_2 atom and the closest F atoms of BF_4^- slightly shortens beyond the uncertainties when the water content increases, although the coordination number does not noticeably change. This shows that the interaction of the C_2···F strengthens with increasing water content. For the distance between the C_4, C_5 atoms and F atoms, the statistical values decrease with increasing water content, but the change in the distance is not so significant beyond the uncertainties. In addition, the number of the C_4···F and C_5···F interactions hardly change with water content. Hence, the weakening of the C_4···F and C_5···F interactions by adding water to $EMI^+BF_4^-$ is not quantitatively cleared by the present LAXS experiments. However, it can be concluded that the C_4···F and C_5···F interactions are not strengthened by addition of water to the ionic liquid.

State and Effect of Water Molecules. The present results of the absorption enthalpies of water, the ATR-IR spectra, and the activation energies for the rotational motion of water molecules clearly show that the state of water molecules changes in the $EMI^+BF_4^-$−water solution at $x_w \approx 0.3$. The ATR-IR spectra for water molecules reveal that water molecules form hydrogen bonds among them in the solutions at the mole fraction, while they exist mainly as isolated molecules in the solutions below the mole fraction. It is very likely that water molecules interact with BF_4^- through hydrogen bonds in the solutions at $x_w \leq \sim 0.3$, as reported in the literature.[9,10,12] Therefore, the rotational motion of water molecules in the solutions observed by the ^2H NMR relaxation measurements is restricted by the hydrogen bonds of BF_4^-···HOH···BF_4^-. However, the hydrogen bond between water molecules and BF_4^- is not strong because of the low negative polarization of fluorine atoms within BF_4^-. In fact, the energy of the hydrogen bond has been estimated to be 9.6 kJ mol^{-1} in the previous study.[8] Thus, another factor should be considered to the restriction for the rotational motion of water. The rigid structure of $EMI^+BF_4^-$ contributes to the restriction of the rotational motion. As seen in Figure 6, the lower the water content, the more the rotational motion of water molecules is retarded in the solutions with lowering temperature. The two factors result in the higher activation energy for the rotational motion than that for bulk water. With increasing water content, on the contrary, the activation energy for the rotational motion of water molecules decreases. This suggests that the second factor slightly decreases; i.e., the inherent structure of $EMI^+BF_4^-$ is gradually loosened with increasing water content, as shown in the LAXS results. In the range of $x_w > \sim 0.3$, however, the activation energy of

the rotational motion of water molecules increases again, resulting from the formation of hydrogen bonds among water molecules. Thus, aggregates of water molecules by hydrogen bonding are formed in the solutions in the low water contents studied. The change in the state of water molecules is reflected into the absorption enthalpies of water estimated from the absorption isotherms. The enthalpies for the $EMI^+BF_4^-$−water system in the range of $x_w < \sim 0.5$ are smaller than that for vaporization of bulk water, while those in the range of $x_w > \sim 0.5$ become larger than the value for bulk water. This shows again that water molecules weakly interact with BF_4^- in the inherent structure of $EMI^+BF_4^-$ in the former, but hydrogen bonds among water molecules are formed in the latter. The inflection point in the absorption enthalpies of water is found at the higher water content of $x_w \approx 0.5$ than those at $x_w \approx 0.3$ in the ATR-IR and NMR results. This may be because water aggregates by hydrogen bonds are grown enough to thermodynamically detect them in the solutions above $x_w \approx 0.5$, while the vibrational and rotational motions of water molecules observed by the ATR-IR and NMR measurements sensitively reflect the formation of hydrogen bonds even in small aggregates, such as dimer of water molecules.

In the above process, as shown in the LAXS results, the inherent structure of $EMI^+BF_4^-$ slightly changes by addition of water up to $x_w = 0.33$. In pure $EMI^+BF_4^-$, the anions of BF_4^- interact mainly with the C_2, C_4, and C_5 atoms of the imidazolium ring. With addition of water to the ionic liquid, the interaction between BF_4^- and the C_2 atom of the imidazolium ring strengthens, whereas those between BF_4^- and the C_4 and C_5 atoms weaken with increasing water content. As seen in the crystal structure of $EMI^+BF_4^-$, the anions of BF_4^- which are close to the C_4 and C_5 atoms of the imidazolium ring may also interact with the C_2 atom of the other neighbor ring. Thus, these findings mean that the numbers of BF_4^- around EMI^+ begin to reduce by addition of water into the ionic liquid. It is likely that water molecules form aggregates by hydrogen bonding as the aggregates intrude into the inherent structure of $EMI^+BF_4^-$. This is due to the much weaker interactions of EMI^+−water and BF_4^-−water than hydrogen bonds among water molecules. The present LAXS experiments clarify that water molecules initiate formation of ion pair of EMI^+ and BF_4^- in the solutions.

The behavior of water molecules in the $EMI^+BF_4^-$−water solutions observed in the present experiments is in good agreement with that in the previous MD simulations.[36,37] The MD results on $EMI^+BF_4^-$−water solution[36] at small water content of $x_w = 0.02$ and 325 K clearly showed that a water molecule is hydrogen-bonded with the fluorine atoms of BF_4^- rather than the hydrogen atom in the imidazolium ring. In spite of the longer alkyl chain of the cation, the MD simulation on $BMI^+BF_4^-$−water solutions[37] at 310 K in the x_w range from 0.111 to 0.5 revealed that water molecules mainly exist as monomer and dimer in the solutions below $x_w = 0.2$, while they form larger aggregates above $x_w = 0.333$. In the solution at $x_w = 0.5$, water aggregates containing more than 10 molecules were observed, and additionally, BF_4^- more strongly interacts with the C_2 atom in the imidazolium ring than the C_4 and C_5 atoms.

Acknowledgment. This work was supported partly by Grant-in-Aid (No. 19550022) from Japan Society for the Promotion of Science. The density measurements and NMR experiments for the sample solutions were carried out at Analytical Research Center for Experimental Sciences of Saga University.

Supporting Information Available: Table S1 for intramolecular interactions of $EMI^+BF_4^-$ and water and Table S2 for all the optimized structure parameters obtained from the LAXS experiments. This material is available free of charge via the Internet at http://pubs.acs.org.

References and Notes

(1) Najdanovic-Visak, V.; Esperancça, J. M. S. S.; Rebelo, L. P. N.; Nunes da Ponte, M.; Guedes, H. J. R.; Seddon, K. R.; de Sousa, H. C.; Szydlowski, J. *J. Phys. Chem. B* **2003**, *107*, 12797.
(2) Wang, J.; Tian, Y.; Zhao, Y.; Zhuo, K. *Green Chem.* **2003**, *5*, 618.
(3) Katayanagi, H.; Nishikawa, K.; Shimozaki, H.; Miki, K.; Westh, P.; Koga, Y. *J. Phys. Chem. B* **2004**, *108*, 19451.
(4) Widegren, J. A.; Saurer, E. M.; Marsh, K. N.; Magee, J. W. *J. Chem. Thermodyn.* **2005**, *37*, 569.
(5) Jarosik, A.; Krajewski, S. R.; Lewandowski, A.; Radzimski, P. *J. Mol. Liq.* **2006**, *123*, 43.
(6) Schröer, W. *J. Mol. Liq.* **2006**, *125*, 164.
(7) Liu, W.; Zhao, T.; Zhang, Y.; Wang, H.; Yu, M. *J. Solution Chem.* **2006**, *35*, 1337.
(8) Cammarata, L.; Kazarian, S. G.; Salter, P. A.; Welton, T. *Phys. Chem. Chem. Phys.* **2001**, *3*, 5192.
(9) Lopez-Pastor, M. L.; Ayora-Canada, M. J.; Valcarcel, M.; Lendl, B. *J. Phys. Chem. B* **2006**, *110*, 10896.
(10) Dominguez-Vidal, A.; Kaun, N.; Ayora-Caada, M. J.; Lendl, B. *J. Phys. Chem. B* **2007**, *111*, 4446.
(11) Jeon, Y.; Sung, J.; Kim, D.; Seo, C.; Cheong, H.; Ouchi, Y.; Ozawa, R.; Hamaguchi, H. *J. Phys. Chem. B* **2008**, *112*, 923.
(12) Zhang, L.; Xu, Z.; Wang, Y.; Li, H. *J. Phys. Chem. B* **2008**, *112*, 6411.
(13) Mele, A.; Tran, C. D.; Lacerda, S. H. D. *Angew. Chem., Int. Ed.* **2003**, *42*, 4364.
(14) Hanke, C. G.; Lynden-Bell, R. M. *J. Phys. Chem. B* **2003**, *107*, 10873.
(15) Kanzaki, R.; Mitsugi, T.; Fukuda, S.; Fujii, K.; Takeuchi, M.; Soejima, Y.; Takamuku, T.; Yamaguchi, T.; Umebayashi, Y.; Ishiguro, S. *J. Mol. Liq.* **2009**, *147*, 77.
(16) Strehmel, V.; Laschewsky, A.; Kraudelt, H.; Wetzel, H.; Goernitz, E. *ACS Symp. Ser.* **2005**, *913* (Ionic Liquids in Polymer Systems), 17.
(17) Bertie, J. E.; Eysel, H. H. *Appl. Spectrosc.* **1985**, *39*, 392.
(18) Yamanaka, K.; Yamaguchi, T.; Wakita, H. *J. Chem. Phys.* **1994**, *101*, 9830.
(19) Ihara, M.; Yamaguchi, T.; Wakita, H.; Matsumoto, T. *Adv. X-Ray Anal. Jpn.* **1994**, *25*, 49. Yamaguchi, T.; Wakita, H.; Yamanaka, K. *Fukuoka Univ. Sci. Rep.* **1999**, *29*, 127.
(20) Furukawa, K. *Rep. Prog. Phys.* **1962**, *25*, 395.
(21) Krogh-Moe, J. *Acta Crystallogr.* **1956**, *2*, 951.
(22) Norman, N. *Acta Crystallogr.* **1957**, *10*, 370.
(23) Takamuku, T.; Tabata, M.; Yamaguchi, A.; Nishimoto, J.; Kumamoto, M.; Wakita, H.; Yamaguchi, T. *J. Phys. Chem. B* **1998**, *102*, 8880.
(24) Johanson, G.; Sandström, M. *Chem. Scr.* **1973**, *4*, 195.
(25) Yamaguchi, T. Doctoral Thesis, Tokyo Institute of Technology, 1978.
(26) Katsyuba, S. A.; Dyson, P. J.; Vandyukoya, E. E.; Chernova, A. V.; Vidis, A. *Helv. Chim. Acta* **2004**, *87*, 2556.
(27) Abragam, A. *The Principles of Nuclear Magnetism*; Oxford University: Oxford, UK, 1961.
(28) Lang, E. W.; Lüdemann, H.-D. In *NMR Basic Principles and Progress*; Springer-Verlag: Berlin, 1990; Vol. 24, pp 130−187.
(29) Struis, R. P. W. J.; De Bleijser, J.; Leyte, C. *J. Phys. Chem.* **1987**, *91*, 1639.
(30) Yasaka, Y.; Wakai, C.; Matubayasi, N.; Nakahara, M. *J. Chem. Phys.* **2007**, *127*, 104506.
(31) Ueno, M.; Ueyama, S.; Hashimoto, S.; Tsuchihashi, N.; Ibuki, K. *J. Solution Chem.* **2004**, *33*, 827.
(32) Choudhury, A. R.; Winterton, N.; Steiner, A.; Cooper, A. I.; Johnson, K. A. *J. Am. Chem. Soc.* **2005**, *127*, 16792.
(33) Matsumoto, K.; Hagiwara, R.; Mazej, Z.; Benkič, P.; Žemva, B. *Solid State Sci.* **2006**, *8*, 1250.
(34) Umebayashi, Y.; Fujimori, T.; Sukizaki, T.; Asada, M.; Fujii, K.; Kanzaki, R.; Ishiguro, S. *J. Phys. Chem. A* **2005**, *109*, 8976.
(35) Ichikawa, K.; Kameda, Y.; Yamaguchi, T.; Wakita, H.; Misawa, M. *Mol. Phys.* **1991**, *73*, 79.
(36) Porter, A. R.; Liem, S. Y.; Popelier, P. L. A. *Phys. Chem. Chem. Phys.* **2008**, *10*, 4240.
(37) Moreno, M.; Castiglione, F.; Mele, A.; Pasqui, C.; Raos, G. *J. Phys. Chem. B* **2008**, *112*, 7826.

JP9042667